Proc. Natl. Acad. Sci. USA
Vol. 96, pp. 6489–6494, May 1999
Pharmacology

Fidelity of G protein β-subunit association by the G protein γ-subunit-like domains of RGS6, RGS7, and RGS11

BRYAN E. SNOW*, LAURIE BETTS†, JOAN MANGION*, JOHN SONDEK†, AND DAVID P. SIDEROVSKI†‡

*Amgen Institute, Toronto, ON, Canada M5G2C1; and †Department of Pharmacology, University of North Carolina, Chapel Hill, NC 27599-7365

Communicated by Alfred G. Gilman, University of Texas Southwestern Medical Center, Dallas, TX, April 8, 1999 (received for review February 25, 1999)

ABSTRACT **Several regulators of G protein signaling (RGS) proteins contain a G protein γ-subunit-like (GGL) domain, which, as we have shown, binds to $G_{\beta 5}$ subunits. Here, we extend our original findings by describing another GGL-domain-containing RGS, human *RGS6*. When RGS6 is coexpressed with different G_β subunits, only RGS6 and $G_{\beta 5}$ interact. The expression of mRNA for *RGS6* and $G_{\beta 5}$ in human tissues overlaps. Predictions of α-helical and coiled-coil character within GGL domains, coupled with measurements of G_β binding by GGL domain mutants, support the contention that G_γ-like regions within RGS proteins interact with $G_{\beta 5}$ subunits in a fashion comparable to conventional G_β/G_γ pairings. Mutation of the highly conserved Phe-61 residue of $G_{\gamma 2}$ to tryptophan, the residue present in all GGL domains, increases the stability of the $G_{\beta 5}/G_{\gamma 2}$ heterodimer, highlighting the importance of this residue to GGL/$G_{\beta 5}$ association.**

The "regulators of G protein signaling" (RGS) protein family consists of at least 20 mammalian gene products that act as GTPase activating proteins on the α-subunits of heterotrimeric, signal-transducing G proteins (1–3). By accelerating the inactivation of GTP-bound G_α subunits, RGS proteins serve as negative regulators of G protein-mediated signaling pathways. Additionally, two RGS proteins, p115–RhoGEF and PDZ–RhoGEF, can also act as effectors, coupling GTP-bound $G_{\alpha 12}$ and/or $G_{\alpha 13}$ to Rho activation (4, 5).

Regions within certain RGS proteins that lie outside the RGS domain interact with other components of G protein signal transduction machinery. For example, the N-terminal PDZ domain of RGS12 associates *in vitro* with the C termini of G protein-coupled receptors (6), and the N-terminal domain of RGS4 mediates receptor-selective inhibition of G protein-mediated Ca^{2+} signaling in pancreatic acinar cells (7). We recently identified a G protein γ subunit-like (GGL) domain within four mammalian RGS family members and identified its role in mediating specific interaction of RGS7 and RGS11 with G protein β5-subunits (8). In a complementary study, a native RGS7/$G_{\beta 5}$ complex has been isolated from bovine retina (9). Our discovery of RGS7/$G_{\beta 5}$ and RGS11/$G_{\beta 5}$ associations tripled the number of known interacting partners for this outlier G_β subunit, which previously had been known to interact only with $G_{\gamma 2}$ (10–13). Here, we describe the cloning, expression, and G_β binding selectivity of RGS6, another RGS protein possessing the GGL domain. Residues critical for G_β subunit binding specificity have been identified by mutagenesis of $G_{\gamma 2}$ and the GGL domains of RGS6, RGS7, and RGS11.

MATERIALS AND METHODS

Expression Constructs. cDNAs for RGS7, RGS11, and G protein subunits have been described (8). RGS6 was isolated by reverse transcription–PCR by using sense (5′-GCG GCC GCA TGG CTC AAG GAT CCG GGG ATC AAA G-3′) and antisense (5′-TCT AGA CTG GGA TCA GGG CCT CTT AGC GAG-3′) primers as described (14) and subcloned with an N-terminal hemagglutinin (HA)-epitope tag into pcDNA3.1 (Invitrogen). G protein β-subunit cDNAs were subcloned with an N-terminal myc-epitope tag into pcDNA3.1 (Invitrogen). Mutagenesis was performed as described (6). The $G_{\gamma 2}$ (F61W)/RGS fusion was created by adding a 17-aa linker (PRAAASVMDICRIRPWYP; derived from pcDNA3.1 polylinker) C-terminal to amino acid 70 of the $G_{\gamma 2}$ (F61W) point mutant, followed by the RGS domain of rat RGS12 (amino acids 716–838; GenBank acc. no. U92280).

***In Vitro* Transcription/Translation.** Reactions were performed, and translation products were immunoprecipitated and analyzed by SDS/PAGE as described (8), except for variations in detergent conditions. "Low-detergent" immunoprecipitations were performed and washed in buffer D [50 mM NaCl/10 mM $MgCl_2$/50 mM Tris, pH 8.0/1 mM EDTA/10 mM 2-mercaptoethanol/20% (vol/vol) glycerol/Complete protease inhibitors; Roche Diagnostics] containing 0.05% C12E10, whereas "high-detergent" immunoprecipitations were performed in buffer D containing 0.1% Triton X-100 and washed in RIPA-500 buffer containing 500 mM NaCl, 1% Triton X-100, 0.5% deoxycholate, and 0.1% SDS.

Transient Transfection and Immunoprecipitation. COS-7 cell lysates were prepared and immunoprecipitated by using RIPA-150 buffer as described (8); proteins were separated by SDS/PAGE, electroblotted onto nitrocellulose, and detected with primary antibodies conjugated to horseradish peroxidase (HRP) and chemiluminescence (Amersham Pharmacia). The HRP-conjugated anti-HA mAb 3F10 was obtained from Roche Diagnostics; HRP-conjugated anti-myc mAb was purchased from Invitrogen.

Model Generation and Analysis. Published alignments (15) allowed for replacement of residues at the interface of $G_{\beta 1}$ and $G_{\gamma 1}$ with the corresponding residues of $G_{\beta 5}$ and the GGL domain of hRGS11 by using the program O (16). Where necessary, alternate allowed rotamers were chosen to limit steric overlap. Conjugate gradient energy minimization of the initial model was done with X-PLOR (17) by using standard energy functions and a coordinate restraint term applied to Cα-positions to compensate for the lack of experimental restraints. Cavity determination was performed by using the program VOIDOO (18). Structures were presented by using INSIGHT (Molecular Simulations, Waltham, MA). Secondary structure and coiled-coil predictions were performed with PREDICTPROTEIN (www.embl-heidelberg.de; ref. 19).

The publication costs of this article were defrayed in part by page charge payment. This article must therefore be hereby marked "*advertisement*" in accordance with 18 U.S.C. §1734 solely to indicate this fact.

PNAS is available online at www.pnas.org.

Abbreviations: ΔD, DEP domain deletion; ΔC, C-terminus deletion; GGL, G protein γ-subunit-like; HA, hemagglutinin; HRP, horseradish peroxidase.

Data deposition: The sequences reported in this paper have been deposited in the GenBank database (accession nos. AF107619 and AF107620).

‡To whom reprint requests should be addressed. e-mail: dsiderov@med.unc.edu.

RESULTS AND DISCUSSION

RGS6 Has a DEP/GGL/RGS Domain Structure and Binds $G_{\beta 5}$. To extend our findings on the G_β binding specificity of RGS7 and RGS11 to other uncharacterized RGS proteins, we cloned human *RGS6*. A partial clone of *RGS6* was described originally as *S194*, a brain-derived mRNA identified during mapping of the human *AD3* locus at chromosome 14q24.3 (20). Database searches with *S194* identified additional human *RGS6* sequence records (e.g., GenBank acc. nos. H09621, AA351873, and AF073920). Oligonucleotides flanking the predicted ORF of full-length *RGS6* were used to amplify *RGS6* mRNA by reverse transcription–PCR from human brain total RNA. Two forms of *RGS6* cDNA were isolated (GenBank acc. nos. AF107619 and AF107620), encoding ORFs of 490 or 472 aa, respectively; the difference between forms is the presence or absence of 18 contiguous amino acids (457-PESEQGRRTSLEKFTRSV-474) C-terminal to the RGS domain, likely a result of alternative splicing.

RGS6 is most similar to RGS7 (21–23). Both RGS6 isoforms encode an N-terminal DEP (*D*isheveled, *E*GL-10, *P*leckstrin) domain (amino acids 39–121) 81% identical to the mouse RGS7 DEP domain, a C-terminal RGS domain (amino acids 333–447) 80% identical to the RGS box of human RGS7, and a GGL domain (amino acids 254–317) 57% identical to the mouse RGS7 GGL domain. In comparison to G_γ subunits, the central portion of the RGS6 GGL domain (amino acids 262–309) is most similar to bovine $G_{\gamma 2}$ (41% identity).

As the RGS7 and RGS11 GGL domains bind only $G_{\beta 5}$ subunits (8), we tested the RGS6 GGL domain for G_β binding specificity. G_β subunits ($G_{\beta 1}$–$G_{\beta 5}$) were produced by *in vitro* transcription/translation along with HA-epitope-tagged RGS proteins or G_γ subunits to detect possible interacting pairs. An anti-HA mAb was used to immunoprecipitate ^{35}S-labeled G_γ and RGS proteins; associated ^{35}S-labeled G_β subunits were detected by SDS/PAGE and autoradiography. $G_{\gamma 2}$ bound to $G_{\beta 1}$, $G_{\beta 2}$, and $G_{\beta 4}$ but not $G_{\beta 5}$ (Fig. 1*A*), as previously described (8, 24). The $G_{\beta 5}/G_{\gamma 2}$ complex is reported to be abnormally sensitive to low levels of detergent compared with other G_β/G_γ pairings (25); we therefore believe that the minimal detergent (0.05% C12E10) necessary during immunoprecipitation results in disruption of the $G_{\beta 5}/G_{\gamma 2}$ complex.

In contrast to the G_β binding specificity of $G_{\gamma 2}$, a truncated RGS6 protein containing both GGL and RGS domains (RGS6ΔDΔC) did not interact with $G_{\beta 1}$–$G_{\beta 4}$ but bound $G_{\beta 5}$, the same specificity observed with the analogously truncated RGS7 (Fig. 1*B*) and RGS11 (see Fig. 3*D* and ref. 8). To determine the specific nature of RGS6/$G_{\beta 5}$ association in a cellular context, COS-7 cells were cotransfected with HA-tagged, full-length RGS6 and one of five myc-tagged G_β subunits. Lysates from transfected cells were immunoprecipitated with anti-HA mAb, and associated G_β subunits were detected with anti-myc antibody. Of the five G_β subunits tested, only $G_{\beta 5}$ coimmunoprecipitated with full-length RGS6 (Fig. 1*C*). We routinely observe greater levels of RGS6 and $G_{\beta 5}$ proteins in cell lysates when they are coexpressed, perhaps reflective of the instability of unpaired G_β and GGL subunits similar to the instability seen in classical G_β and G_γ subunits (26–28), including $G_{\beta 5}$ (11).

We conclude that, within the DEP/GGL/RGS subfamily of RGS proteins, RGS6 is most closely related to RGS7 in primary sequence and shares $G_{\beta 5}$ binding selectivity with both RGS7 and RGS11.

RGS6 and $G_{\beta 5}$ mRNAs Have Overlapping Distribution. Unlike the widespread expression of other G_β subunits, $G_{\beta 5}$ mRNA is expressed in a tissue-restricted manner: mouse $G_{\beta 5}$ is expressed predominantly in the brain and retina (10, 29), whereas human $G_{\beta 5}$ mRNA is found in brain, retina, kidney, and pancreas (8, 30). To test whether *RGS6* and $G_{\beta 5}$ are coexpressed in human tissues, we compared expression patterns of both genes in Northern blot analyses. *RGS6* mRNA was detected in whole brain (Fig. 2 *A* and *B*) and in brain anatomical regions with an expression pattern overlapping that of $G_{\beta 5}$; however, *RGS6* expression is barely detectable in the caudate putamen and spinal cord (Fig. 2*C*). This pattern of expression is in contrast with that reported by Gold *et al.* (31) for *RGS6* in the rat brain; such a cross-species difference in brain expression patterns also was observed for *RGS11* (8, 31). Unlike the expression pattern of human *RGS11*, human *RGS6* mRNA is not seen in the retina or pancreas but is observed in the heart (Fig. 2 *A* and *B*). The observed coexpression of *RGS6* and $G_{\beta 5}$ mRNA in the human brain suggests that an RGS6/$G_{\beta 5}$ complex may play a role in G protein-mediated neuronal signaling.

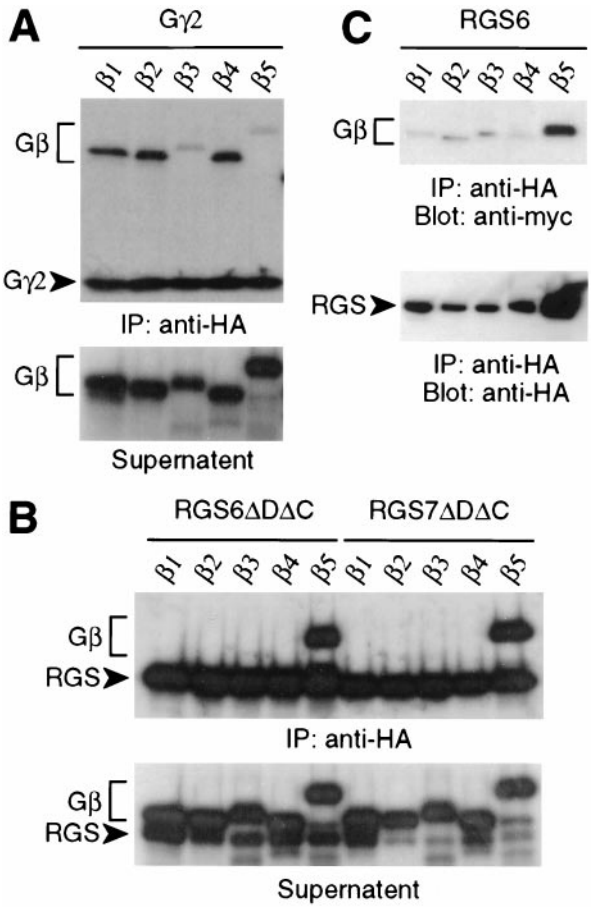

FIG. 1. G_β binding specificity of RGS6 and RGS7. G_β subunits were cotranslated in reticulocyte lysates with (*A*) HA-tagged $G_{\gamma 2}$ or (*B*) HA-tagged, truncated RGS6 (ΔDΔC, where ΔD indicates a DEP domain deletion and ΔC indicates a C-terminal deletion; amino acids 255–456) or truncated RGS7 (ΔDΔC; amino acids 202–395, SwissProt P49802) protein. Lysates were immunoprecipitated (IP) in low detergent with anti-HA mAb, and immunoprecipitated proteins and clarified supernatants were visualized separately by SDS/PAGE and autoradiography. (*C*) Expression vectors for full-length, HA-tagged RGS6 and individual, myc-tagged G_β subunits were transiently cotransfected into COS-7 cells. Cell lysates were immunoprecipitated with anti-HA mAb, and coimmunoprecipitated G_β subunits were detected by immunoblotting (Blot) with anti-myc-HRP or anti-HA-HRP conjugates.

GGL Domain Fidelity: Testing the "Trp-274 Hypothesis." An assumption inherent in our original report (8) is that sequence homology between GGL domains and G_γ subunits reflects a similarity at the secondary and quaternary structure levels—i.e., a predominantly α-helical extended chain forming extensive contacts, including an N-terminal parallel coiled coil (15), with $G_{\beta 5}$ subunits. Indeed, secondary structure predic-

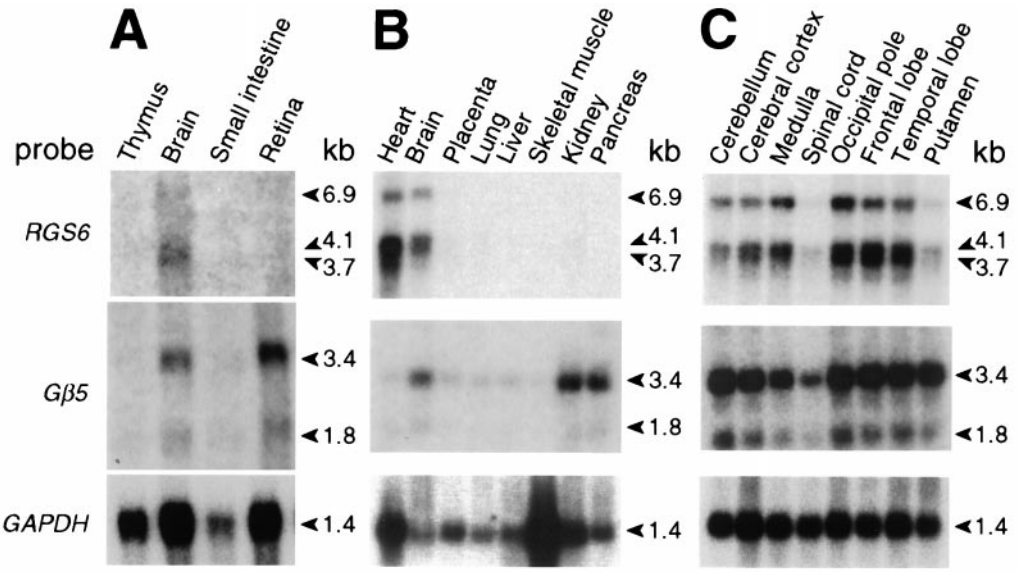

FIG. 2. Comparison of *RGS6* and $G_{\beta 5}$ expression patterns. Northern blots of 20 μg total RNA (*A*) or 2 μg poly(A+) RNA from various human tissues (*B* and *C*) were serially hybridized with a $G_{\beta 5}$ cDNA probe (ref. 8), with a glyceraldehyde-3-phosphate dehydrogenase (GAPDH) cDNA probe as a control for RNA loading and quality, and with an *RGS6* cDNA probe. kb, kilobase.

tions for RGS6 (Fig. 3*A*), RGS7, and RGS11 (data not shown) suggest an α-helical character in regions analogous to the first two α-helices of $G_{\gamma 1}$ and $G_{\gamma 2}$ (15, 32); for the RGS9 GGL domain, only the N-terminal region (amino acids 216–233) is predicted to be α-helical (data not shown). Furthermore, for both RGS6 and RGS7, the putative N-terminal α-helix within the GGL domain is predicted to participate in a coiled-coil structure (Fig. 3*A* and data not shown); its putative counterpart, the N terminus of $G_{\beta 5}$, is also predicted to form a coiled coil by the same program (ref. 33; data not shown).

In our initial report (8), we predicted an important role for Trp-274 of the RGS11 GGL domain in $G_{\beta 5}$ selectivity (the Trp-274 hypothesis), given that (*i*) all G_γ subunits have a smaller aromatic residue (Phe) at the analogous position and (*ii*) $G_{\beta 1}$–$G_{\beta 4}$ have a larger residue (Asn-340) than that of $G_{\beta 5}$ (Ala-353) at the position predicted to interact with Trp-274 of RGS11 (8). To test this prediction, we created GGL-domain mutants by replacing tryptophan with phenylalanine in RGS6 (W309F), RGS7 (W306F), and RGS11 (W274F) and assessed G_β binding by coexpression with $G_{\beta 1}$–$G_{\beta 5}$ *in vitro*. None of the Trp-to-Phe mutants acquired affinity toward $G_{\beta 1}$–$G_{\beta 4}$ (Fig. 3 *B–D*), and the mutations had only a modest impact on $G_{\beta 5}$ affinities in low-detergent conditions (0.05% C12E10). However, the Trp-to-Phe mutations destabilized the GGL/$G_{\beta 5}$ interactions in high-detergent conditions; for example, when washed with 1% Triton X-100/0.1% SDS/0.5% sodium cholate, very little $G_{\beta 5}$ remained bound to the W274F mutant of RGS11 (Fig. 3*E*, lane 3) in comparison to robust $G_{\beta 5}$ binding observed for the wild-type protein (Fig. 3*E*, lane 1). Similarly destabilized $G_{\beta 5}$ interactions were observed with RGS6 and RGS7 Trp-to-Phe mutants in high-detergent conditions (data not shown). This region is clearly critical for G_β binding, as mutation of tryptophan and the preceding proline to serine and alanine, respectively, eliminates $G_{\beta 5}$ binding by RGS11 (PW274AS; Fig. 3*D*). This result is entirely consistent with the known importance of this dipeptide motif in the $G_{\beta 1}/G_{\gamma 1}$ and $G_{\beta 1}/G_{\gamma 2}$ crystal structures, in which the proline "kinks" the Cα-chain inward toward $G_{\beta 1}$, positioning the phenylalanine residue into a hydrophobic pocket (15, 32).

GGL Domain Fidelity: Role of Other Residues. Other amino acids within RGS6 and RGS11 were also modified, singly or in tandem, to test their roles in both $G_{\beta 5}$ binding affinity and G_β subunit binding selectivity. Ser-245 of RGS11 and Asp-297 of RGS6 represent two positions conserved among all GGL domains and G_γ subunits (8). The analogous positions within $G_{\gamma 1}$ (Ser-34 and Asp-51) and $G_{\gamma 2}$ (Ser-31 and Asp-48) form hydrogen bonds with Asp-27 and Ser-279/Ser-281 of $G_{\beta 1}$, respectively (15, 32). Conversion of Ser-245 (RGS11) and Asp-297 (RGS6) to alanine confirmed their importance to GGL domain function; considerably reduced $G_{\beta 5}$ binding was seen with the RGS11 S245A mutant (Fig. 3*F*), whereas the RGS6 D297A mutant did not bind $G_{\beta 5}$ at all, either *in vitro* (Fig. 3*B*) or in cell cotransfection studies (data not shown). In contrast, Gln-271 of RGS6 is conserved only in the highly related RGS7; as expected, mutation of Gln-271 to alanine (the residue present within RGS9 and RGS11) had no discernable effect on $G_{\beta 5}$ binding by RGS6 (Fig. 3*B*).

Gln-257 of RGS11 is conserved among all GGL domains, including that of EGL-10 (8), whereas the analogous position within $G_{\gamma 1}$ (Glu-46) and $G_{\gamma 2}$ (Ala-43) is neither well conserved nor involved in interactions with $G_{\beta 1}$ (15, 32). Hence, as predicted by the lack of importance to G_γ/G_β interactions, replacement of Gln-257 with alanine yielded no change in the G_β binding behavior of RGS11 (Q257A; Fig. 3*F*). To this point, therefore, GGL domain mutations affect GGL/$G_{\beta 5}$ assembly when made in positions analogous to G_γ/G_β contact points. Conversely, GGL domain mutations do not affect GGL/$G_{\beta 5}$ assembly when made in positions analogous to those not involved in G_γ/G_β contacts. These findings support our assumption that the GGL domain interacts with $G_{\beta 5}$ in a manner similar to conventional G_γ/G_β pairings.

GGL Domain Fidelity: Comparison to $G_{\gamma 1}$'s Selectivity for $G_{\beta 1}$. Studies of $G_{\gamma 1}$ and $G_{\gamma 2}$ binding specificities have identified a five-residue region of $G_{\gamma 1}$ (amino acids 36–40) critical for selective dimerization with $G_{\beta 1}$ and not $G_{\beta 2}$ (34, 35); replacement of three residues of $G_{\gamma 1}$, Cys-36–Cys-37–Glu-38, with the corresponding residues of $G_{\gamma 2}$, Ala-33–Ala-34–Ala-35, is sufficient to allow binding of $G_{\gamma 1}$ to $G_{\beta 2}$ (35). Therefore, we replaced the corresponding residues of RGS11 (Cys-247–Leu-248–Glu-249) with three alanines and tested G_β subunit association. The triple-alanine mutation, either alone (CLE249AAA) or in combination with mutation to Trp-274 (W274F + CLE249AAA; not shown), neither engendered additional G_β binding specificity nor abrogated association with $G_{\beta 5}$ (Fig. 3*F*) and $G_{\beta 5L}$ (data not shown), suggesting that, unlike $G_{\gamma 1}$ and $G_{\gamma 2}$, this region of the GGL domain does not control G_β binding selectivity.

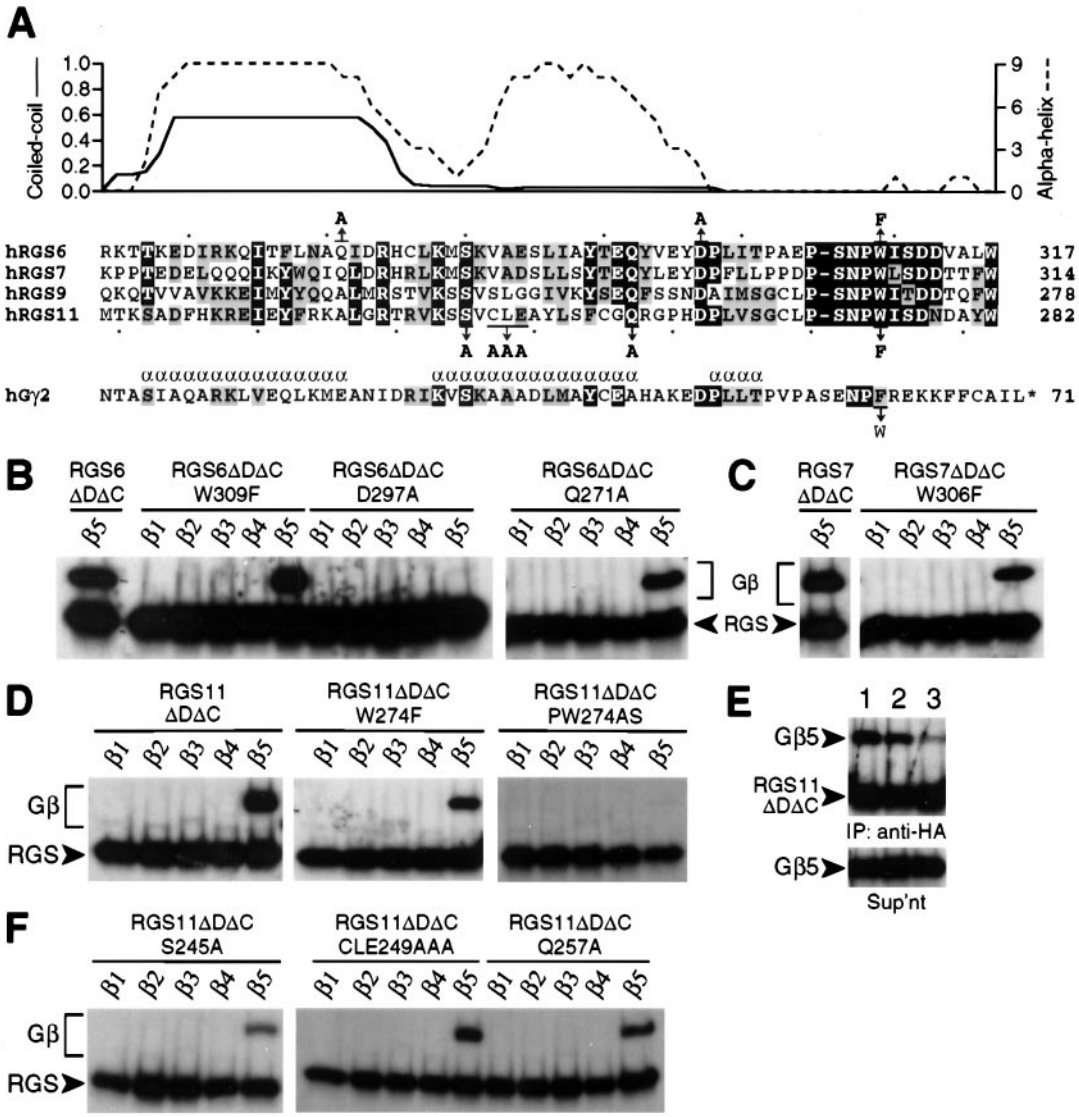

FIG. 3. *In vitro* G_β binding specificity of GGL domain mutants. (*A*) Secondary structure predictions for the RGS6 GGL domain and sequence alignment between $G_{\gamma 2}$, RGS6, RGS7, RGS9, and RGS11. Identical residues are in black boxes; conserved residues are shown in shaded boxes. For RGS6, probabilities of α-helical character (indexed to a maximum of 9; ref. 19) and coiled-coil interaction (indexed to a maximum of 1.0; ref. 33) are plotted above the primary sequence of the GGL domain (*x* axis). α-Helices within $G_{\gamma 2}$ (ref. 32) are indicated by an α above the sequence. The position and nature of point mutations are denoted above or below the sequence line with arrows. Individual G_β subunits were cotranslated in reticulocyte lysates with wild-type or mutant RGS6 (*B*), RGS7 (*C*), and RGS11 proteins (*D–F*). HA-tagged RGS or G_γ proteins were immunoprecipitated in low detergent (except as noted in *E*) with anti-HA mAb, and associated G_β proteins were visualized by SDS/PAGE and autoradiography. (*E*) Immunoprecipitations (IP) of cotranslated $G_{\beta 5}$ and wild-type (lane 1) or W274F mutant (lanes 2 and 3) RGS11ΔDΔC proteins were performed in high-detergent (lanes 1 and 3) or low-detergent (lane 2) conditions and visualized separately from clarified supernatants (Sup'nt) as above.

Fidelity of $G_{\gamma 1}$ and $G_{\gamma 2}$: Revisiting the Trp-274 Hypothesis. We tested a corollary of the Trp-274 hypothesis espoused above; namely, that conversion of the analogous position within $G_{\gamma 1}$ and $G_{\gamma 2}$ from phenylalanine to tryptophan would prevent or weaken binding to $G_{\beta 1}$–$G_{\beta 4}$ and/or allow $G_{\beta 5}$ association. The G_β binding characteristics of $G_{\gamma 1}$ were unaffected by this mutation (F64W), as compared with wild-type $G_{\gamma 1}$ (Fig. 4*A*). In contrast, the same mutation to $G_{\gamma 2}$ (F61W), although it did not affect affinity toward $G_{\beta 1}$–$G_{\beta 4}$, engendered binding to $G_{\beta 5}$ when tested *in vitro* in low-detergent conditions (Fig. 4*A*). Under high-detergent conditions, $G_{\beta 5}$ binding was not detected, whereas binding to other G_β subunits was unaffected [$G_{\gamma 2}$ (F61W) RIPA-500 vs. C12E10; Fig. 4*A*].

Of all mutants tested for $G_{\beta 5}$ interaction, only the $G_{\gamma 2}$ (F61W) mutant and the cognate GGL domain Trp-to-Phe mutants were affected by detergent conditions; all other GGL domain mutants (Fig. 3*A*) had the same affinity (or lack thereof) for $G_{\beta 5}$ isoforms in cotranslation studies with low- or high-detergent conditions (data not shown). We believe this detergent sensitivity explains our inability to detect $G_{\beta 5}$ binding by $G_{\gamma 2}$ (F61W) after exposure to RIPA-150 buffer in cell cotransfection experiments (Fig. 4*B*). This conclusion is consistent with the extreme detergent sensitivity of the wild-type $G_{\beta 5}/G_{\gamma 2}$ complex (25). Additionally, *in vitro* cotranslation/immunoprecipitation studies with high-detergent RIPA-500 buffer disrupt RGS7/$G_{\beta 5}$ association in contrast to robust interaction observed in low-detergent conditions (Fig. 1*B* and data not shown). The *in vitro* association of RGS6 and RGS11 with $G_{\beta 5}$ isoforms has far more tolerance to high-detergent conditions, allowing for detection of such complexes upon COS-7 cotransfection and RIPA-buffer lysis (Fig. 1*C* and ref. 8).

Lack of Steric Hindrance from the RGS Domain. To test the possibility that GGL-domain-containing RGS proteins are

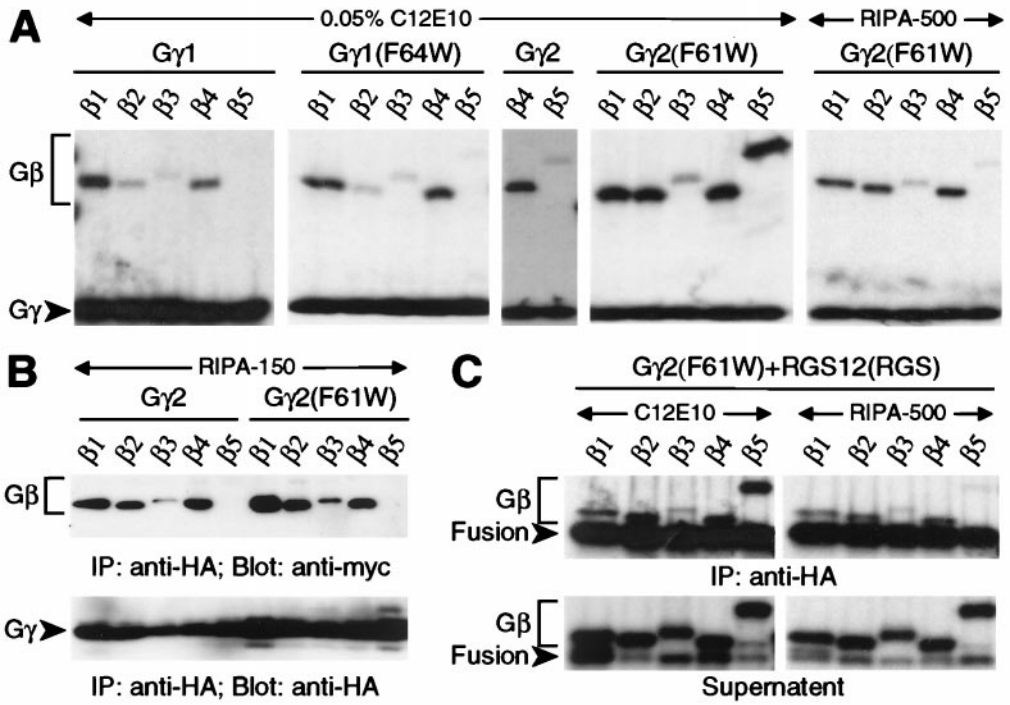

FIG. 4. G_β binding specificity of $G_{\gamma 1}$ and $G_{\gamma 2}$ mutants. HA-tagged G_γ proteins (wild-type or mutated as indicated) were either cotranslated *in vitro* (*A* and *C*) or cotransfected into COS-7 cells (*B*) with individual G_β subunits, immunoprecipitated (IP) with anti-HA mAb in either low detergent (0.05% C12E10) or high detergent (RIPA), and visualized by SDS/PAGE and autoradiography (*A* and *C*) or immunoblotting (*B*) with indicated antisera (Blot). "Fusion" denotes chimeric protein composed of HA-tagged $G_{\gamma 2}$ (F61W) subunit fused to the rat RGS12 RGS domain.

prevented from binding $G_{\beta 1}$–$G_{\beta 4}$ because of steric hindrance from a C-terminal RGS domain absent in conventional G_γ subunits, we created a chimeric $G_{\gamma 2}$ (F61W)/RGS protein that mimics the spatial orientation of GGL and RGS domains. As observed for the $G_{\gamma 2}$ (F61W) protein, the larger $G_{\gamma 2}$ (F61W)/RGS12 fusion protein associated with $G_{\beta 1}$, $G_{\beta 2}$, $G_{\beta 4}$, and $G_{\beta 5}$ subunits *in vitro* in low-detergent conditions, with a loss only of $G_{\beta 5}$ association apparent in high-detergent conditions (Fig. 3*C*). This result suggests that the lack of interaction between $G_{\beta 1}$–$G_{\beta 4}$ subunits and GGL-domain-containing RGS proteins is not the result of steric hindrance from the RGS domain but rather is intrinsic to the GGL domain.

Molecular Modeling of the Interaction of RGS11 Trp-274 with $G_{\beta 5}$. To understand the role of the Trp-274 position in differential G_β binding affinities of GGL domains and G_γ subunits, we returned to our RGS11/$G_{\beta 5}$ interface model (8), which is based on side-chain replacement of the $G_{\beta 1}/G_{\gamma 1}$ crystal coordinates (15). The highlighted $G_{\beta 5}$/GGL interface (Fig. 5*B*) has greater complementarity than the equivalent region in $G_{\beta 1}/G_{\gamma 1}$ (Fig. 5*A*). In the $G_{\beta 1}/G_{\gamma 1}$ crystal structure

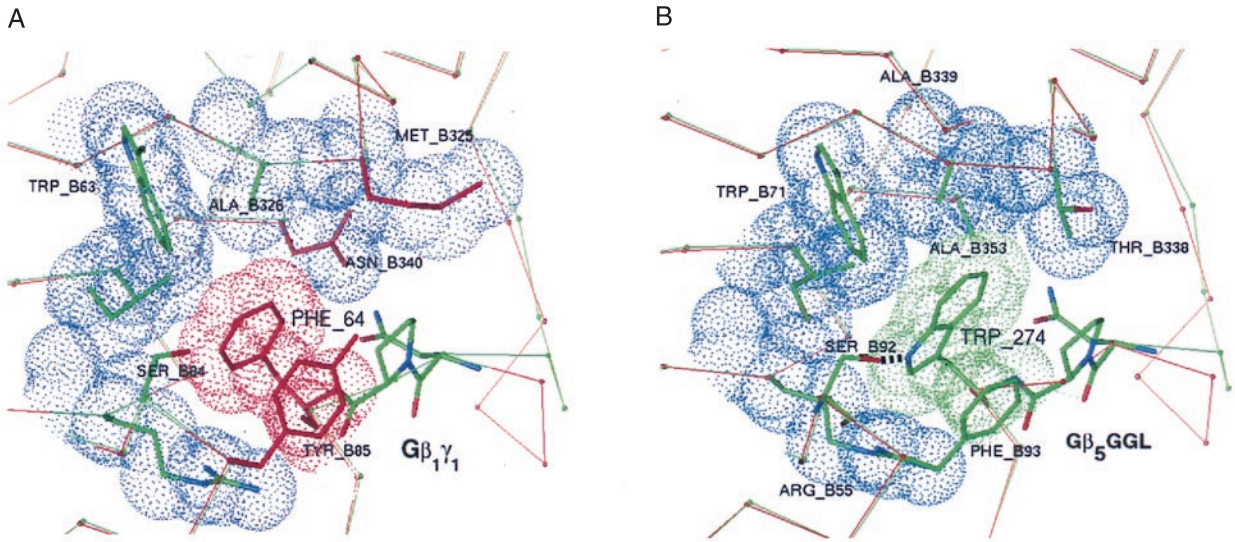

FIG. 5. Specificity-determining residues at the interface of $G_{\beta 1}$ and $G_{\gamma 1}$ compared with equivalent regions of modeled $G_{\beta 5}$ and the GGL domain of RGS11. Highlighted in blue are van der Waals surfaces of $G_{\beta 1}$ contacting Phe-64 of $G_{\gamma 1}$ (*A*) or similar contacts between $G_{\beta 5}$ and Trp-274 of the RGS11 GGL domain (*B*). Residues colored red in the $G_{\beta 1}/G_{\gamma 1}$ structure differ from equivalent residues in the $G_{\beta 5}$/GGL model. Except for the conserved tripeptide motif (NPF or NPW), thin red and green lines trace the Cα-backbone of $G_{\beta 1}/G_{\gamma 1}$ and $G_{\beta 5}$/GGL, respectively. Just before the conserved tripeptide motif, the Cα-traces diverge because of the insertion of a single residue in $G_{\gamma 1}$ relative to the GGL domain.

(15), packing defects around Phe-64 produce a ≈3.0-Å^3 cavity, whereas no equivalent cavity surrounds Trp-274 in the modeled $G_{\beta5}$/GGL complex. In addition, Thr-338 and Ala-353 in $G_{\beta5}$ are smaller than the corresponding residues of $G_{\beta1}$ (Met-325 and Asn-340) and serve to accommodate the larger bulk of Trp-274 relative to Phe-64. Further enhancing the specificity of the $G_{\beta5}$/GGL complex, the hydroxyl group of Ser-92 in $G_{\beta5}$ potentially forms a hydrogen bond with the indole nitrogen of Trp-274; no similar hydrogen bond is possible in the $G_{\beta1}/G_{\gamma1}$ structure.

The presence of a small cavity in $G_{\beta1}/G_{\gamma1}$ around Phe-64 suggests that this pocket could accommodate a larger residue, thereby allowing $G_{\gamma1}$ (F64W) and $G_{\gamma2}$ (F61W) mutants to maintain binding to their normal G_β partners (Fig. 4*A*). If this pocket within $G_{\beta5}$ specifies a Trp residue in GGL domains by virtue of increased cavity size and potential hydrogen bonding with Ser-92, then this specification could partially explain why $G_{\gamma2}$ (F61W) has increased affinity for $G_{\beta5}$ as a binding partner. The reverse mutation to Phe in the GGL domain would not fit as snugly into the pocket specifying Trp, thereby giving a relative loss of binding energy, which was observed as lowered *in vitro* affinity for $G_{\beta5}$ by RGS6(W309F), RGS7(W306F), and RGS11(W274F) under high-detergent conditions. We await experimentally derived structural data on the GGL/$G_{\beta5}$ complex to confirm the relative importance of this region to G_β binding specificity.

We extend our discovery of a GGL domain within RGS7 and RGS11 to include RGS6. Structural predictions and mutagenesis data strengthen our belief that the GGL domain binds to $G_{\beta5}$ subunits in a manner similar to that of conventional G_β/G_γ associations. The molecular basis for the absolute selectively of the GGL domain for $G_{\beta5}$ subunits remains to be determined. However, we have been able to increase the relative strength of the $G_{\beta5}/G_{\gamma2}$ association by mutating a single residue within $G_{\gamma2}$, Phe-61. This mutation is presumed to mimic atomic interactions unique to wild-type $G_{\beta5}$/GGL domain associations. Continued study of the nature of $G_{\beta5}$ association by GGL domains relative to that of Gγ subunits should assist our understanding of the role(s) of the DEP/GGL/RGS proteins in modulating G protein-coupled signaling.

Note. While this manuscript was under review, two additional reports of RGS/$G_{\beta5}$ association were published (36, 37). One reported the discovery of a tight association between RGS9 and $G_{\beta5L}$ in rod photoreceptors (36). This discovery validates our original prediction based on the presence of a GGL domain within the primary sequence of RGS9.

1. Siderovski, D. P., Hessel, A., Chung, S., Mak, T. W. & Tyers, M. (1996) *Curr. Biol.* **6,** 211–212.
2. Dohlman, H. G. & Thorner, J. (1997) *J. Biol. Chem.* **272,** 3871–3874.
3. Berman, D. M. & Gilman, A. G. (1998) *J. Biol. Chem.* **273,** 1269–1272.
4. Hart, M. J., Jiang, X., Kozasa, T., Roscoe, W., Singer, W. D., Gilman, A. G., Sternweis, P. C. & Bollag, G. (1998) *Science* **280,** 2112–2114.
5. Fukuhara, S., Murga, C., Zohar, M., Igishi, T. & Gutkind, J. S. (1999) *J. Biol. Chem.* **274,** 5868–5879.
6. Snow, B. E., Hall, R. A., Krumins, A. M., Brothers, G. M., Bouchard, D., Brothers, C. A., Chung, S., Mangion, J., Gilman, A. G., Lefkowitz, R. J., *et al.* (1998) *J. Biol. Chem.* **273,** 17749–17755.
7. Zeng, W., Xu, X., Popov, S., Mukhopadhyay, S., Chidiac, P., Swistok, J., Danho, W., Yagaloff, K. A., Fisher, S. L., Ross, E. M., *et al.* (1998) *J. Biol. Chem.* **273,** 34687–34691.
8. Snow, B. E., Krumins, A. M., Brothers, G. M., Lee, S.-F., Wall, M. A., Chung, S., Mangion, J., Arya, S., Gilman, A. G. & Siderovski, D. P. (1998) *Proc. Natl. Acad. Sci. USA* **95,** 13307–13312.
9. Cabrera, J. L., de Frietas, F., Satpaev, D. K. & Slepak, V. Z. (1998) *Biochem. Biophys. Res. Commun.* **28,** 898–902.
10. Watson, A. J., Aragay, A. M., Slepak, V. Z. & Simon, M. I. (1996) *J. Biol. Chem.* **271,** 28154–28160.
11. Zhang, S., Coso, O. A., Lee, C., Gutkind, J. S. & Simonds, W. F. (1996) *J. Biol. Chem.* **271,** 33575–33579.
12. Bayewitch, M. L., Avidor-Reiss, T., Levy, R., Pfeuffer, T., Nevo, I., Simonds, W. F. & Vogel, Z. (1998) *J. Biol. Chem.* **273,** 636–644.
13. Lindorfer, M. A., Myung, C.-S., Savino, Y., Yasuda, H., Khazan, R. & Garrison, J. C. (1998) *J. Biol. Chem.* **273,** 34429–34436.
14. Snow, B. E., Antonio, L., Suggs, S. & Siderovski, D. P. (1998) *Gene* **206,** 247–253.
15. Sondek, J., Bohm, A., Lambright, D. G., Hamm, H. E. & Sigler, P. B. (1996) *Nature (London)* **379,** 369–374.
16. Jones, T. A. & Kjeldgard, M. (1996) O (Dept. Cell Mol. Biol., Uppsala Univ., Uppsala), Version 6.1.
17. Brunger, A. T. (1993) X-PLOR (Dept. Mol. Biophys. Biochem., Yale Univ., New Haven, CT), Version 3.1.
18. Kleywegt, G. J. & Jones, T. A. (1994) *Acta Crystallogr. D* **50,** 178–185.
19. Rost, B. (1996) *Methods Enzymol.* **266,** 525–539.
20. Sherrington, R., Rogaev, E. I., Liang, Y., Rogaeva, E. A., Levesque, G., Ikeda, M., Chi, H., Lin, C., Li, G., Holman, K., *et al.* (1995) *Nature (London)* **375,** 754–760.
21. Koelle, M. R. & Horvitz, H. R. (1996) *Cell* **84,** 115–125.
22. He, W., Cowan, C. W. & Wensel, T. G. (1998) *Neuron* **20,** 95–102.
23. Elmore, T., Rodriguez, A. & Smith, D. P. (1998) *DNA Cell Biol.* **17,** 983–989.
24. Yan, K., Kalyanaraman, V. & Gautam, N. (1996) *J. Biol. Chem.* **271,** 7141–7146.
25. Fletcher, J. E., Lindorfer, M. A., Defilippo, J. M., Yasuda, H., Guilmard, M. & Garrison, J. C. (1998) *J. Biol. Chem.* **273,** 636–644.
26. Schmidt, C. J. & Neer, E. J. (1991) *J. Biol. Chem.* **266,** 4538–4544.
27. Pronin, A. N. & Gautam, N. (1993) *FEBS Lett.* **328,** 89–93.
28. Higgins, J. B. & Casey, P. J. (1994) *J. Biol. Chem.* **269,** 9067–9073.
29. Watson, A. J., Katz, A. & Simon, M. I. (1994) *J. Biol. Chem.* **269,** 22150–22156.
30. Jones, P. G., Lombardi, S. J. & Cockett, M. I. (1998) *Biochim. Biophys. Acta* **1402,** 288–291.
31. Gold, S. J., Ni, Y. G., Dohlman, H. G. & Nestler, E. J. (1997) *J. Neurosci.* **17,** 8024–8037.
32. Wall, M. A., Posner, B. A. & Sprang, S. R. (1998) *Structure (London)* **6,** 1169–1183.
33. Lupas, A., Van Dyke, M. & Stock, J. (1991) *Science* **252,** 1162–1164.
34. Lee, C., Murakami, T. & Simonds, W. F. (1995) *J. Biol. Chem.* **270,** 8779–8784.
35. Meister, M., Dietrich, A. & Gierschik, P. (1995) *Eur. J. Biochem.* **234,** 171–177.
36. Makino, E. R., Handy, J. W., Li, T. & Arshavsky, V. Y. (1999) *Proc. Natl. Acad. Sci. USA* **96,** 1947–1952.
37. Levay, K., Cabrera, J. L., Satpaev, D. K. & Slepak, V. Z. (1999) *Proc. Natl. Acad. Sci. USA* **96,** 2503–2507.